

Self-diffusion of particles in gas-driven granular layers with periodic flow modulation

C. S. Orellana,^{1,2} I. S. Aranson,¹ W.-K. Kwok,¹ and S. Rica²

¹Materials Science Division, Argonne National Laboratory, 9700 South Cass Avenue, Argonne, Illinois 60439, USA

²Departamento de Física, Universidad de Chile, Blanco Encalada 2008, Santiago 6511226, Chile

(Received 28 July 2005; published 17 October 2005)

We study self-diffusion of particles in gas-driven granular layers by high-speed fluorescent video microscopy. We show that periodic flow modulation results in an enhancement of the particle's diffusion. The diffusion enhancement, which in turn is an indication of more efficient fluidization of the granular layer, is associated with the onset of disordered subharmonic patterns. Our measurements provide a sensitive characterization method of the fluidization properties of particulate-gas systems.

DOI: [10.1103/PhysRevE.72.040301](https://doi.org/10.1103/PhysRevE.72.040301)

PACS number(s): 45.70.Mg, 45.70.Qj

The properties of gas-driven particulate systems are the subject of intensive research in the engineering community [1,2]. Fluidized beds, consisting of a vertical column energized by the flow of gas or liquid pumped through the bottom, are widely used in industry for mixing, catalysis, and combustion. Fluidization occurs when the drag force exerted by the fluid on the granulate exceeds gravity. A uniform fluidization, the most desirable regime for most industrial applications, turns out to be prone to bubbling instabilities: bubbles of clear fluid created at the bottom traverse the granular layer and destroy the uniform fluidization state [2]. The instability of the gas-fluidized beds is prompted by non-equilibrium gas-solid interaction and accelerated by dissipation induced by particle collision [3,4]. The control and suppression of bubble instabilities are two of the most discussed issues in the engineering community [2,5–7]. A variety of approaches for gas solid systems have been proposed, including mechanically vibrated beds [8,9], ultrasonic wave fluidization [10], and pulsed gas flow [11].

Recently gas-driven granular layers have attracted the attention of the physics community as interesting well-controlled granular systems with short-range particle collisions mediated by nonlocal interaction with the surrounding fluid and driven by a nontrivial mechanism [12–14]. In our previous work (Ref. [12]) we studied a shallow gas-fluidized bed subjected to periodic air-flow modulations. We found a sequence of well-defined transitions between disordered states dominated by spontaneous bubbling fluidization and ordered states with periodic subharmonic patterns as the frequency, the amplitude of modulation, and the flow rate were varied. Whereas our system displayed many similarities with the spontaneous pattern formation in vertically vibrated granular layers [15–18], there were also important differences. For example, the variation of the mean flow rate is equivalent to the variation of gravity, which is certainly not easy to achieve in the above experiments. Moreover, our studies indicated that the formation of periodic patterns results in the suppression of large bubbles, and thus, possibly to improvement of fluidization and particulate-gas contact.

In this paper we focus on the quantitative characterization of the fluidized state in the presence of periodic flow modulations. The efficiency of fluidization is characterized by the particle's self-diffusion, which in turn is related to the effective viscosity of the particulate-gas mixture. Using high-

speed ultraviolet (UV) fluorescent video microscopy, we performed experimental studies of tracer particle's diffusion in gas-fluidized granular layers. We find that the particle's diffusion is enhanced with the formation of disordered subharmonic patterns.

The schematic of the experiment is shown in Fig. 1. The experimental cell is built of transparent Plexiglas and has an inner diameter of 140 mm. To ensure high uniformity of the flow, the bottom of the bed is made of a sintered porous brass plate with an average pore size of 60 μm ; packed plastic rings are used for initial flow redistribution. For the most part, the experiments were conducted using spherical glass particles with a diameter between 0.15 and 0.18 mm. We used a granular layer thickness h of 1.5 mm, i.e., about ten particle diameters. For tracer particles we used 0.2 mm yellow light fluorescent spheres (SPHEROTECH, No. FP-200052-0.2g). Dry air is pumped through the plate, and the flow rate is controlled by a proportional valve with a response time below 0.004 sec. The surface of the granular

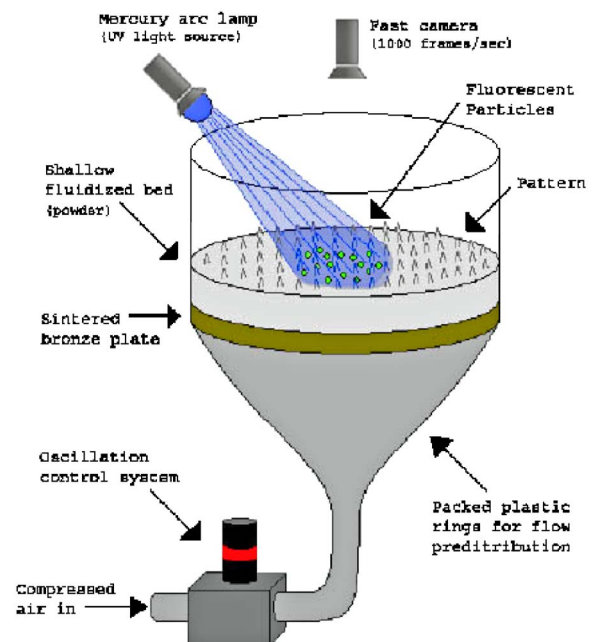


FIG. 1. (Color online) Schematics of the experimental setup.

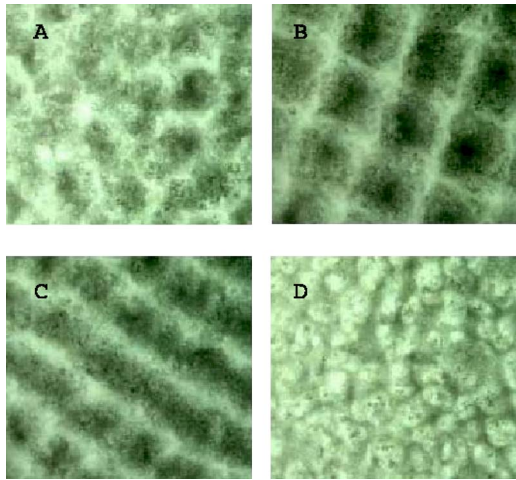


FIG. 2. (Color online) Representative patterns observed experimentally: (a) short-range order pattern ($f=17$ Hz), (b) squares ($f=19$ Hz), (c) stripes ($f=21$ Hz), and (d) Turbulent bubbling ($f=25$ Hz) for mean flow rate 10.3 cm/s and amplitude of flow modulation 5.2 cm/s.

layer is illuminated with a powerful UV light source (mercury arc lamp). To trace the markers, a high-speed digital camera (up to 1000 frames per second) was set up to detect only the light emitted by the fluorescent marker particles (mostly in the green range). Since we used a bed of transparent glass particles, we were able to track our markers even *below* the surface of the bed. We tracked as many as 20 particles simultaneously for a relatively long time in a variety of fluidization regimes—from the onset of fluidization to highly turbulent states. Since our markers are only slightly larger than the glass particles comprising the bed, we believe that the diffusive behavior of the markers provide a faithful characterization of the particle's self-diffusion.

In our previous work (Ref. [12]) we found that periodic flow modulation may result in the formation of a variety of subharmonic patterns depending on the modulation parameters, the depth of the layer, and the mean gas flow rate. Select patterns are shown in Fig. 2. In this work, we focus on the effects which large-scale patterns have on the self-diffusion of the particles. To measure the diffusion coefficient, we extracted the particle's positions from image sequences obtained through high-speed video analysis. The mean square displacement \mathbf{r}_i for each particle was extracted with the aid of a Matlab image-processing toolbox. In order to accumulate sufficient statistics, we tracked up to 20 particles in each frame. The particle's self-diffusion coefficient D was defined as

$$\langle \mathbf{r}^2 \rangle = 4Dt \quad (1)$$

where t is time. The average was taken for all particles and from several experimental sequences. Typical particle trajectories for different types of large-scale patterns are shown in Fig. 3. The anisotropic character of the particle's diffusion is noticeable for the square patterns. The Brownian character of the particle's motion can be illustrated by the probability density function $P(\mathbf{r}, t)$ to find the particle at the position \mathbf{r} at

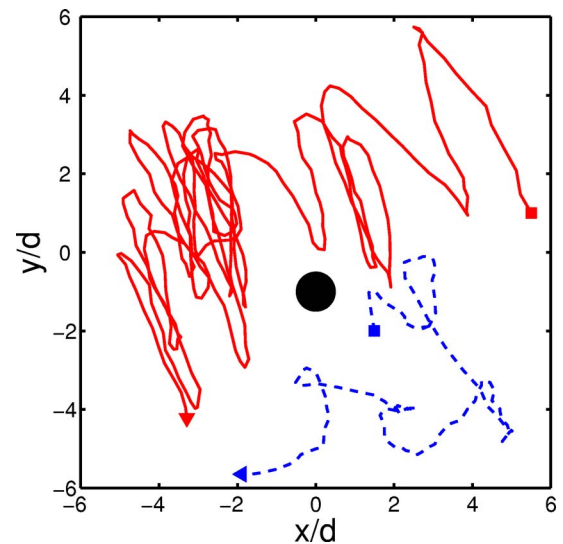


FIG. 3. (Color online) Representative particles trajectories for 19 Hz (solid line, square pattern) and 17.5 Hz (dashed line, short-range pattern).

the moment of time t . Since in two-dimensional diffusion processes, $P(\mathbf{r}, t) \sim t^{-1} \exp[-r^2/(4Dt)]$, the radial distribution function $P(r, t)$ is of the form

$$P(r, t) \sim r \exp\left(-\frac{r^2}{4Dt}\right). \quad (2)$$

Figure 4 shows $P(r)$ for some fixed time $t=t^*=0.04$ sec. The best fit to Eq. (2) coincides with the experimental data within the thickness of the line. Thus, our results support Brownian motion of the particles. Similarly, the radial velocity distribution function is also consistent with Gaussian law, see Fig. 5. The occurrence of Brownian motion in our nonequilibrium system can be interpreted as manifestation of some sort of "effective temperature" defined from the width of velocity distribution function, see Fig. 5. This effective temperature is

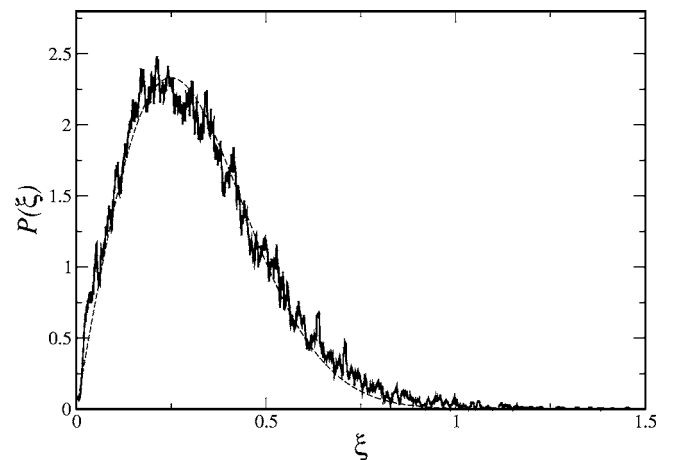


FIG. 4. Radial probability density $P(\xi)$ at $t=t^*=0.04$ sec for $f=19$ Hz (square pattern) vs $\xi=r/d$, d is particle's diameter. Dashed line shows best fit to Gaussian law $P \sim \xi \exp[-\xi^2/4\tilde{D}]$, with normalized diffusion $\tilde{D} \approx 1/32$.

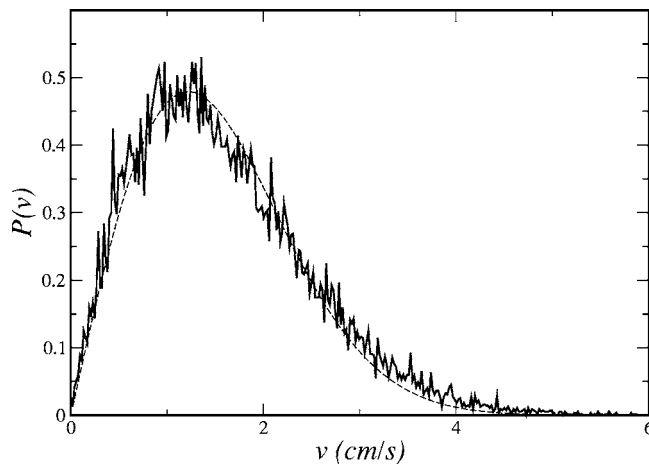


FIG. 5. Radial velocity distribution $P(v)$ for $f=18$ Hz, mean flow rate 10.3 cm/sec and modulation amplitude 5.23 cm/sec. Dashed line shows best fit to Gaussian law $P \sim v \exp[-\zeta v^2]$ with $\zeta \approx 0.33$.

likely different from kinetic granular temperature defined as mean squared fluctuation particles velocity. The concept of Brownian motion and connection to the fluctuation-dissipation relation in air-fluidized [14] and dense driven granular flows was recently explored in Refs. [19] and [20]. In this context, we emphasize that Brownian motion is a natural occurrence in our situation since we consider a rather energized *granular liquid*, whereas Refs. [19] and [20] focused on a slow dense granular flow where the connections to thermodynamics and to the concept of “effective temperature” are less obvious and debatable. It could be very interesting to test directly the applicability of the Einstein-Stokes relation theorem in a gas fluidized system in the broad range of flow regimes by independent measurements of the particles’ self-diffusion and the viscous drag force.

We systematically studied the dependence of the diffusion coefficient D as a function of modulation parameters and mean flow rate. The results are summarized in Fig. 6. As it follows from Fig. 6, the dependence of D against flow parameters is highly nonmonotonous. The general trend is a noticeable increase in diffusion with the formation of large-scale patterns. In particular, in Fig. 6 the peak at $f=17$ Hz is associated with the onset of disordered (short-range) subharmonic patterns, see Fig. 2(a). Surprisingly, well-developed square patterns for $f=19-20$ Hz are characterized by a smaller diffusion coefficient. Similar, but somewhat smaller peaks are observed for the transition to stripes at higher frequency. In this case of regular periodic patterns (stripes and squares), the diffusion happens to be anisotropic, e.g., the diffusion parallel to the stripe and perpendicular to the stripe happens to be different. This effect can be explained by the fact that the diffusion of particles between elementary cells of a periodic square pattern is significantly suppressed, and the large-scale diffusion occurs mostly along the square pattern antinodal lines, similar to the situation considered in Ref. [21]. In contrast, for the disordered states appearing for lower frequency ($f=17$ Hz), the particles are advected all over the cell and the essentially isotropic large-scale flows increase the diffusion.

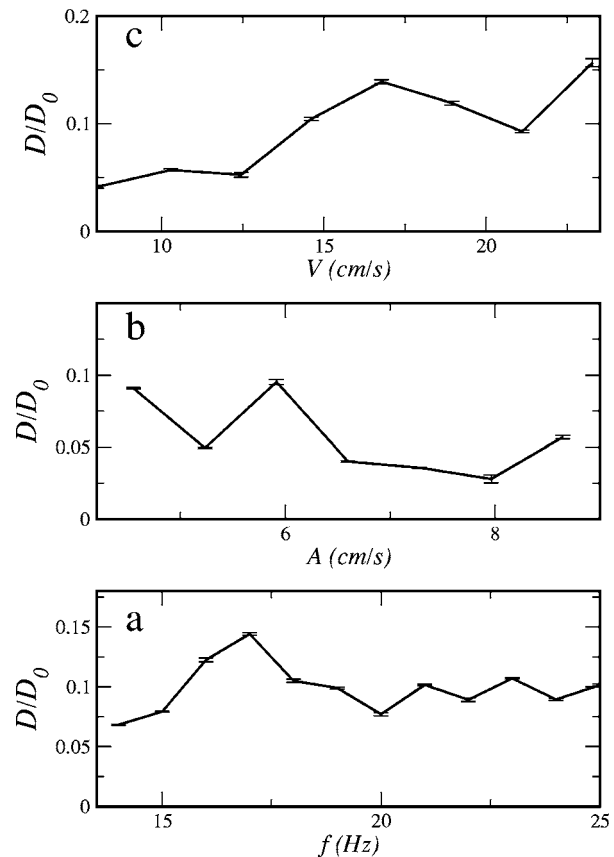


FIG. 6. Diffusion coefficient D vs modulation parameters and flow rate. (a) D vs f , mean flow is $V=10.3$ cm/s and the amplitude is $A=5.2$ cm/s. (b) D vs amplitude, $f=19$ Hz and the mean flow is 10.3 cm/s. (c) D vs mean flow rate, $f=19$ Hz and the amplitude 7.8 cm/s. Turbulent bubbling occurs for $V>20$ cm/sec. The diffusion D is normalized by $D_0=Vd$, where $d=0.15$ mm is the particle size.

The diffusion coefficient provides a sensitive characterization of the efficiency of the fluidization process and of the particulate-gas contact in our system. In our previous work (Ref. [12]) the enhancement of fluidization was associated with the decrease in pressure drop across the granular layer, which in most cases was rather small (a few percent). In contrast, there is a considerable increase in the particle’s self-diffusion associated with the formation of large-scale coherent patterns. Alternatively, the increase in diffusion can be interpreted as a decrease in the effective viscosity of the particulate-gas mixture and an increase of the effective temperature, which is directly connected to the “microscopic” properties of the fluidized state. A larger diffusion coefficient also implies more homogeneous and efficient mixing.

In conclusion, we performed experimental studies of a particle’s self-diffusion in gas-fluidized beds with periodic flow modulations. Our studies revealed a considerable increase of the diffusion coefficient related to the onset of large-scale pattern formation. The diffusion measurements provide a sensitive tool for the characterization of the fluidized state. Our results give insights into the physics of driven granular systems with complex interactions. Alternatively,

our method can be used to test and validate various molecular dynamics simulation codes for gas-fluidized particles systems, and consequently, differentiate continuum models of multiphase flows. Our studies also provide directions for the control and suppression of bubbling instabilities in gas-fluidized beds.

We thank Vitalii Vlasko-Vlasov, Jie Li, and Alexey Snchezko for help. This research was supported by the U.S. Department of Energy Grant No. W-31-109-ENG-38. The support of Fundación Andes of Chile, Fondecyt 1020359 and Fondap 11980002 of Chile (C.S.O. and S.R.) is acknowledged.

-
- [1] D. Kunii and O. Levenspiel, *Fluidization Engineering* (Butterworth, Boston, 1991); J. R. Grace, A. A. Avidan, and T. M. Knowlton, *Circulating Fluidized Beds* (Blackie Acad. & Prof., London, 1997).
- [2] R. Jackson, in *Fluidization*, edited by J. F. Davidson, R. Clift, and D. Harrison (Academic, London, 1985).
- [3] J. Li and J. A. M. Kuipers, *Chem. Eng. Sci.* **58**, 711 (2003).
- [4] B. P. B. Hoomans, J. A. M. Kuipers, W. J. Briels, and W. P. M. van Swaaij, *Chem. Eng. Sci.* **51**, 99 (1996).
- [5] B. J. Glasser, S. Sundaresan, and I. G. Kevrekidis, *Phys. Rev. Lett.* **81**, 1849 (1998).
- [6] J. M. Valverde, A. Castellanos, and M. A. Sanchez Quintanilla, *Phys. Rev. Lett.* **86**, 3020 (2001).
- [7] S. Sundaresan, *Annu. Rev. Fluid Mech.* **35**, 63 (2003).
- [8] K. Noda, Y. Mawatari, and S. Uchida, *Powder Technol.* **99**, 11 (1998).
- [9] B. Thomas, M. O. Mason, R. Sprung, and Y. A. Liu, *Powder Technol.* **99**, 293 (1998).
- [10] R. Chirone, L. Massimilla, and S. Russo, *Chem. Eng. Sci.* **48**, 41 (1993).
- [11] H. W. Wong and M. H. I. Baird, *Chem. Eng. J.* **2**, 104 (1971).
- [12] J. Li, I. S. Aranson, W.-K. Kwok, and L. S. Tsimring, *Phys. Rev. Lett.* **90**, 134301 (2003).
- [13] M. Schröter, D. I. Goldman, and H. L. Swinney, *Phys. Rev. E* **71**, 030301(R) (2005).
- [14] R. P. Ojha *et al.*, *Nature (London)* **427**, 521 (2004); R. P. Ojha, A. R. Abate, and D. J. Durian, *Phys. Rev. E* **71**, 016313 (2005); A. R. Abate and D. J. Durian, *ibid.* **72**, 031305 (2005).
- [15] F. Melo, P. Umbanhowar, and H. L. Swinney, *Phys. Rev. Lett.* **72**, 172 (1994); F. Melo, P. B. Umbanhowar, and H. L. Swinney, *Phys. Rev. Lett.* **75**, 3838 (1995); P. B. Umbanhowar, F. Melo, and H. L. Swinney, *Nature (London)* **382**, 793 (1996).
- [16] I. S. Aranson *et al.*, *Phys. Rev. Lett.* **82**, 731 (1999).
- [17] C. Bizon, M. D. Shattuck, J. B. Swift, W. D. McCormick, and H. L. Swinney, *Phys. Rev. Lett.* **80**, 57 (1998).
- [18] L. S. Tsimring and I. S. Aranson, *Phys. Rev. Lett.* **79**, 213 (1997); I. S. Aranson, L. S. Tsimring, and V. M. Vinokur, *Phys. Rev. E* **59**, R1327 (1999).
- [19] H. A. Makse and J. Kurchan, *Nature (London)* **415**, 614 (2002).
- [20] G. D'Anna, P. Mayor, A. Barrat, V. Loreto, and F. Nori, *Nature (London)* **424**, 909 (2003).
- [21] W. Young, A. Pumir, and Y. Pomeau, *Phys. Fluids A* **1**, 462 (1989).